

# Assessment of the optical efficiency of a primary lens to be used in a CPV system

Marta Victoria <sup>\*</sup>, Stephen Askins, Rebeca Herrero, Ignacio Antón, Gabriel Sala

## A B S T R A C T

This article summarizes experimental methods to evaluate the performance and to assess the efficiency of a lens that will be used as primary optics in a concentrating photovoltaic system comprising multijunction solar cells. The methods are classified into two groups: those intended to quantify the transmission losses and those that estimate the size and shape of the light spot. In addition, the optical efficiency definition is reviewed and a systematic procedure to evaluate it is proposed.

## 1. Introduction

As the title suggests, the issue addressed in this article is not the evaluation of the efficiency of a generic lens, but it is limited to the measurement of primary optics that will be included in concentrating photovoltaic (CPV) systems. The requirements of CPV are therefore taken into account when defining the lens optical efficiency and how it should be measured. CPV systems generally use multijunction (MJ) solar cells based on semiconductors from groups III and V. These cells use the solar spectrum more effectively to achieve efficiencies that double that of typical silicon solar cells. To counteract the higher cost of MJ devices they are used under light concentrated several hundred times by an optical system. The concentrating optics are composed of lenses or mirrors. Refractive systems, in particular Fresnel lenses, are the most common in modern CPV systems, usually manufactured using poly (methyl methacrylate) (PMMA) or silicone on glass (SOG).

At the current stage of CPV development, there is a need to standardize both optical efficiency definition and measuring methods, in order to allow fair and accurate comparison among different technologies. The analysis of the lens performance would help the designer to identify the optimum working conditions, particularly the maximum geometric concentration achievable (which impact on the cost through the cell size) and to assess the appropriateness of a second optical stage (Victoria et al., 2009) which can potentially improve the optical performance but also the system cost.

In particular the definition of optical efficiency, that of the whole optical system or any of its component, is crucial to improve the communication among optics and systems designers and manufacturers. As a first step, this article focuses exclusively on the efficiency measurement of a standard component of CPV systems: the primary lens. It also seeks to contribute to the ongoing discussions within IEC TC 82 Workgroup 7 to draft a Technical Specification for CPV primary optics. Additionally, reliable and reproducible efficiency measurements are mandatory to assess the degradation of lenses. In fact, this last point is one of the main concerns related to CPV: its ability to remain working outdoors for more than 25 years without showing significant degradation. To discriminate if the optical system has been degraded it is imperative to provide methods that allow the measurement and comparison of the lens efficiency initially and at different moments throughout its lifetime.

Over the last years, the CPV systems group at the Solar Energy Institute of the Technical University of Madrid (IES-UPM) has accumulated substantial experience in the characterization of CPV optics. A review of characterization procedures for CPV systems, independently of any receiver, and providing the necessary parameters for the design of a system was already published in 2003 (Antón et al., 2003). Nevertheless that work was very focused on single junction solar cells, prevailing at that time, and since then, the emergence of the MJ cells demands a deeper characterization of spectral issues caused by refractive primary optics. In the last decade we had the opportunity of measuring several kinds of lenses from different manufacturers, including PMMA and SOG technologies, whose sizes range from  $2.5 \times 2.5$  cm to  $32 \times 32$  cm.

Significant results from those experiments and descriptions of the methods have been previously reported in several articles (Antón et al., 2003; Askins et al., 2011; Herrero et al., 2012). This paper aims to show this knowledge in a more comprehensive and systematic way to make it more useful to the reader.

The article is organized as follows. First, Sections 2 and 3 review the factors affecting the performance of a lens and the definition of optical efficiency. Subsequently, Sections 4 and 5 gather the proposed measuring methods highlighting the main sources of error that should be monitored. In particular, Tables 1 and 2 summarize all the experimental methods at a glance. Section 6 presents an example of all the data that would be reported following the optical characterization of a lens. Finally, in the last section, we recommend some of the methods over the others and justify our selection. Before proceed we should remark that we are limiting ourselves, at this stage, to the efficiency measurement of individual lenses. As a consequence, the description of procedures to evaluate the variation in the performance of lens parquets are beyond the scope of this article.

## 2. Factors affecting the performance of a CPV lens

The phenomena that affect the optical efficiency of a lens can be organized into two groups. On one side, those which lower the throughput of radiant power through the lens: absorption in the lens material, reflections at any of the lens faces, losses due a large number of grooves and their draft angles, high-angle Lambertian scattering at the interfaces, etc. In general, these parameters will have the same effect on the system optical efficiency regardless of the size of the receiver (in other words, the geometric concentration ratio it is to be operated at) and the type of solar cell. Light affected by these parameters is simply lost. On the other side, we find characteristics that affect the spectral and spatial irradiance distribution at the lens focus: chromatic aberration, the width of the Fresnel grooves, low-angle scattering due to surface quality, lack of flatness or other manufacturing errors, and temperature effects. These characteristics affect where the light goes (that is, how well the lens acts as a concentrator) and therefore their effect on overall system optical efficiency is, to a greater or lesser degree, dependent of the receiver and cell properties, from the simply area of the device (which determines the geometric concentration ratio) to more complex technological parameters such as the distribution of the series resistance throughout the device (Espinete, 2012; Kurtz and O'Neill, 1996; Victoria et al., 2013) (see Fig. 1).

Therefore, to fully characterize a given lens for any possible CPV application, we propose to separate these two classes of lens characteristics into two separate parameters: *effective optical efficiency* and *effective concentration ratio*. Since the former should be independent of the latter, it is crucial that it is measured with an irradiance sensor at the focal plane of the lens that is large enough to capture every ray. This is especially critical if we intend to measure the optical efficiency for different lens-to-receiver distances. For example, if we want to evaluate the performance of the off-focused lens. Off-focus here means that the receiver is closer or further from the lens than its nominal position and it is an easy method to imitate the performance of the lens when it is warmer or colder than its nominal temperature. Based on our previous experience, to measure the *effective optical efficiency* we recommend using a sensor such that the geometric concentration is lower than 50 $\times$ . Notice that for the largest lenses used currently in the industry, which have an area of approximately 0.1 m<sup>2</sup>, a sensor with at least 5  $\times$  5 cm active area is required.

In the following sections we describe several proposed lens characterization methods and classify them according to their aim; either to assess the transmittance losses or to estimate the

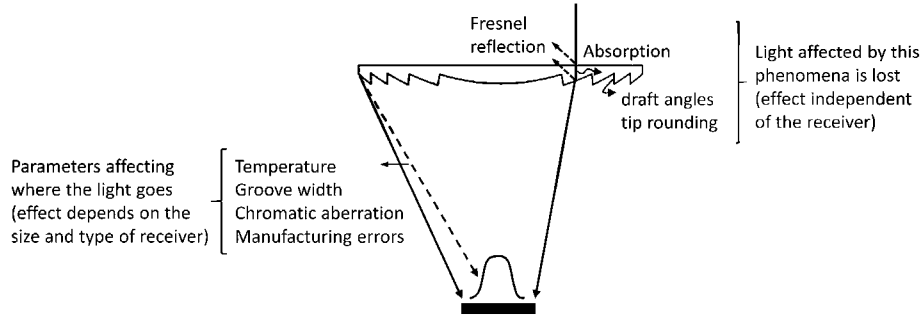
**Table 1** Experimental methods and main associated sources of error for the estimation of an optical efficiency value.

Method	Characteristics		Main sources of error								
	Irradiance & spectrum control	Lens temperature	Temperature affects the sensor (if no active cooling)	Sensor/solar cell size	Linearity, non-uniformity effects	Front metallization grid shading factor	Angular distribution over the cell	Subcell limitation (if solar cell)	Solar simulator uniformity	Response too slow for a flash-light source	
Thermal irradiance sensor	Outdoors Indoors	x	x	x	x				x	x	
Solar cell as irradiance sensor	Outdoors, Si/MJ solar cell	x	x	x	x	x	x	x			
	Indoors, Si/MJ solar cell			x	x	x	x	x	x		
Wavelength resolved efficiency (spectroradiometer)	Outdoors Indoors	x	x	x	x				x	x	

**Table 2**

Experimental methods and main associated sources of error for the quantification of the size of the light spot.

Quantifying the size of the light spot								
Method	Characteristics	Main sources of error						
		Solar cell size	Linearity, no-uniformity effects	Front metallization shading factor	Angular distribution over the cell/sensor	Solar simulator uniformity	Spectral mismatch (CCD sensor vs. solar cell)	Background noise (image processing)
Encircled energy by using solar cells of different sizes	Indoors	x	x	x	x	x		
Lambertian diffusor and CCD camera	Indoors					x	x	x

**Fig. 1.** Schematic representation of the main phenomena affecting the efficiency of a primary lens.

size, the spatial or the spectral distribution of the spot. Tables 1 and 2 present a general overview of the experimental methods and the main sources of error identified.

### 3. Definition of optical efficiency

The *optical efficiency*  $\eta_{op}$  of a lens illuminated by a given light source can be defined as the fraction of radiant power at its input aperture  $P_{in}$  which reaches its output  $P_{out}$  (Antón et al., 2003). The efficiency can be expressed in terms of the average irradiance at the input lens aperture  $G_{in}(\theta, \lambda)$ , the output irradiance at the lens focus  $G_{out}(\theta, \lambda)$  and the geometric concentration  $X_{geo}$ . The geometric concentration is defined as the ratio of the input area  $A_{in}$  (i.e., area evaluated at the input aperture of the lens) to the output area  $A_{out}$  (i.e., area evaluated at the focal plane of the lens or, what is equivalent, the receiver area).

$$\eta_{op} = \frac{P_{out}}{P_{in}} = \frac{G_{out}A_{out}}{G_{in}A_{in}} = \frac{G_{out}}{G_{in}X_{geo}} \quad (1)$$

This definition is extremely intuitive but, if it is applied to actually measure the efficiency of a CPV lens, there are several aspects that must be carefully considered because it is strongly dependent on the light source characteristics and type of irradiance sensors used to measure both  $G_{in}(\theta, \lambda)$  and  $G_{out}(\theta, \lambda)$ . In the first place, the definition of efficiency is closely related to  $X_{geo}$ . The estimated value will be different if we use a large receiver or if instead the evaluated output area is too small and some light is not captured by it. This statement may seem obvious but it is one of the major sources of error in the efficiency measurement. Probably if we have in mind a particular CPV system we will be interested in evaluating the efficiency for the corresponding concentration  $X_{geo}$ . Secondly, although  $G_{in}(\theta, \lambda)$  is represented in Eq. (1) by a single value, it depends on the angular and spectral features of the light impinging the entrance. Therefore, in order to perform an indoor measurement, the light source should be angularly and spectrally equivalent to the real Sun to obtain a representative value for CPV applications. In the third place, insofar as the response of the

sensor used to measure  $G_{out}(\theta, \lambda)$  depends on the angular and spectral distribution of the light at the focus of the lens, the optical efficiency is also dependent on such characteristics. An ideal irradiance sensor should have a flat spectral response and a cosine angular response to account for the total power transmitted by the lens.

A more practical definition of the optical efficiency for a CPV lens can be introduced if solar cells are used as receiver, i.e., as irradiance sensor. In this case, the spectral response  $SR(\lambda)$  of the solar cell weights the significance of every wavelength  $\lambda$ , and both  $G_{in}$  and  $G_{out}$  can be estimated by measuring the photocurrent of a pair of identical solar cells illuminated by the light at the lens entrance (*IN*) and at its focus (*OUT*) respectively:

$$G_{in} = \frac{I_{sc}^{IN}}{I_{sc}^{IN}(1)} 1000 \text{ W/m}^2 \quad (2)$$

$$G_{out} = \frac{I_{sc}^{OUT}}{I_{sc}^{OUT}(1)} 1000 \text{ W/m}^2 \quad (3)$$

where  $I_{sc}^{IN}(1)$  and  $I_{sc}^{OUT}(1)$  are the calibrated values of the photocurrent of the two solar cells under a reference irradiance (typically at 1 sun or  $1000 \text{ W m}^{-2}$  under the reference spectrum AM1.5D-G173-03).

Thus, an optical efficiency, referred to as *effective optical efficiency*  $\eta_{op,eff}$ , can be formulated which accounts for the transmission of 'effective' radiant power, i.e., it compares the photocurrent produced by the light transferred to the cell to that produced by the cell if it were exposed to the same light flux at the lens aperture.

$$\eta_{op,eff} = \frac{G_{cell}}{G_{in}X_{geo}} = \frac{I_{sc}^{OUT} I_{sc}^{IN}(1)}{I_{sc}^{IN} I_{sc}^{OUT}(1) X_{geo}} \quad (4)$$

The solar cells used as light sensors, particularly the one used at the exit of the lens, must accomplish several requirements to ensure accuracy: linearity of the current response with the concentration level, a lack of current dependence with the non-uniform

irradiance patterns produced by the lens, an angular response wider than the cone of light cast by the lens, to name a few. In other words, the transmittance of the solar cell must be the same when the light impinges normal to its surface (one-sun measurement) as when it receives concentrated light. For primary lenses commonly used in CPV systems these conditions are met because they usually show  $f$ -numbers large enough ( $f$ -number  $> 1.1$ , cone semi-angle  $< 25^\circ$ ) to avoid significant losses due to Fresnel reflection and TIR losses at the second surface. Additionally, since the impinging light must be highly collimated (similar to the Sun), the solar cell used to measure the input irradiance must be inside a collimating tube (Chai, 1976) in order to avoid stray light and to ensure that only direct irradiance is measured.

As most CPV systems comprise MJ solar cells, we may use them as irradiance sensors for the  $\eta_{op,eff}$  measurement. MJ solar cells are composed of several series-connected subcells, each with a different bandgap to convert a specific part of the solar spectrum. The lowest generating subcell limits the current of the device, so several effective optical efficiencies, one per subcell, can be considered. Consequently, an additional requirement is to ensure that the subcell limiting the current is the same for the device at the lens aperture (that measures  $G_{in}$ ) and at the lens exit (that measures  $G_{out}$ ). When the lens-to-receiver distance is slightly modified due to chromatic aberration the subcell limiting the current may change causing an error in the efficiency measurement. Using 'isotype' cells is an option to overcome this problem. An 'isotype' or component cell is equivalent to a MJ solar cell in which only one of the subcells is electrically connected. Hence, it behaves optically as a MJ solar cell but the photogenerated current corresponds to the connected subcell regardless of the spectral distribution of the incident light. In this way the effective lens efficiency  $\eta_{op,eff,subcell i}$  can be estimated for each subcell  $i$  comprising the photovoltaic device to be used.

$$\eta_{op,eff,subcell i} = \frac{G_{out,subcell i}}{G_{in,subcell i} X_g} = \frac{I_{sc,subcell i}^{OUT} I_{sc,subcell i}^{IN}(1)}{I_{sc,subcell i}^{IN} I_{sc,subcell i}^{OUT}(1) X_g} \quad (5)$$

The main drawback of this approach is, of course, that it requires having large area 'isotype' cells. They can sometimes be supplied by the MJ solar cells manufacturer but they are quite expensive and not always available at the needed area.

An alternative solution consists in using the subcell-limitation diagrams to estimate the short-circuit current for every subcell. This experimental method is explained in detailed elsewhere (Domínguez et al., 2013). It allows the determination of every subcell photocurrent by taking advantage of a large variation in the light spectrum, for example throughout the pulse decay of a Xenon lamp of a CPV solar simulator. It also requires a set of 'isotype' cells whose spectral response is similar to that of the MJ solar cell to be used in the final CPV system. However, in this approach it does not matter the size of the 'isotype' cells and the same set can be used for measuring different lens.

## 4. Measuring methods to evaluate the optical efficiency of a lens

### 4.1. Characterization of the optical efficiency – thermal irradiance sensors

To determine the *optical efficiency*, irradiance sensors with a broadband and flat spectral response that collects every wavelength of interest are needed to measure the irradiance at the lens input aperture  $G_{in}$  and at the lens output  $G_{out}$ . Irradiance sensors based on thermopiles are a simple option. However, its angular acceptance must be adequately modified to measure only direct irradiance at the optics aperture. While a simple pyrheliometer is very adequate for measuring  $G_{in}$ , the main difficulty relies on

finding a sensor large enough to measure  $G_{out}$ , with a cross-calibration to the pyrheliometer. Consequently, a challenging requirement is the linearity of the  $G_{out}$  sensor, since at the lens aperture it receives uniform irradiance at around one sun, while at the exit the lens creates a non-uniform irradiance distribution reaching at the center several times the average concentration. A possible solution to avoid losing linearity consists in adding neutral density filter (i.e. mesh filters) to reduce the irradiance level at the output surface. In this case, the transmittance of the filter must be known and discounted, increasing the uncertainty of the measurement.

If the measurement is performed outdoors, under real Sun, the spectral distribution of the light must be monitored, e.g., using a spectroradiometer. In addition, we must check that the heating of the sensor under concentrated light does not modify its spectral response. The temperature of the lens also needs to be controlled since, for certain materials, this parameter has a strong influence on the lens performance (Rumyantsev et al., 2010; Hornung et al., 2010; Askins et al., 2011). Nevertheless, the main drawback that disallows the outdoor measurement is the fact that the Sun may not be available when needed. Indoor measurement can be carried out using a CPV solar simulator. Since the response of a thermal sensor is too slow for any flash-light source, the method can only be applied to steady-state solar simulators. Considering the extreme difficulty of manufacturing such solar simulators due to the light requirements (high collimation and irradiance, control of light spectrum, size of the beam larger than the primary lens and heat dissipation for the continuous source) leads us to the next proposed method where this limitation is avoided.

### 4.2. Characterization of the effective optical efficiency – solar cell as irradiance sensor

When a solar cell is used to measure the irradiance at the focal plane of the lens,  $G_{out}$  is weighted by the spectral response of the cell. Considering the irradiance level needed (up to 100 suns on average) and the size of the receiver (for the largest lenses,  $5 \times 5$  cm), a silicon solar cell designed for such concentration level is probably the best option. An identical cell (identical relative spectral response) can be used to quantify the irradiance at the lens aperture  $G_{in}$ , but it should be placed inside a collimating tube to ensure that it only measure direct irradiance. For the same reason care should be taken to ensure that the only light reaching the cell when measuring  $G_{out}$  is that projected by the lens, and not stray light or reflections from the solar simulator source. The two solar cells need to have identical spectral responses, including the transmittance of any antireflective coating (ARC) or encapsulant (either bare cell or glass and silicone cover) employed. In order to attain an accurate and reproducible measurement it must be ensured that: (1) the solar cell size is large enough to collect every ray projected by the lens, (2) the photoresponse of the solar cell is linear between one sun and the working concentration level, (3) the transmittance at the cell entrance is the same under normal irradiance and when a cone of light impinges the cell – ARC angular dependence must be carefully analyzed, (4) the non-uniform irradiance distribution over the cell does not affect the device photocurrent, and (5) the different effective shading-factors caused by the front metallization grid when the cell is uniformly illuminated and when it is under the lens do not affect the result. In some cases, the receiver cell must be slightly reverse biased to measure the photocurrent or neutral filters (e.g., mesh filters) may be needed to limit the concentration level.

Concerns related to outdoors measurements stated in the previous section apply here. The irradiance and spectral distribution of the light must be monitored and the lens temperature must be controlled. If a continuous source is used, the variation in the solar

cell spectral response when it heats up due to concentrated irradiance must be taken into account as well.

Indoor measurements can be carried out using a flash based CPV solar simulator such as the Helios 3198 (Domínguez et al., 2008). Its illumination system comprises a large-area parabolic mirror and a Xenon strobe at its focus. The angular size and spectral distribution equivalent to the real Sun can be attained adding a large integrating sphere into this scheme. Figs. 2 and 3 show the indoor measuring set-up at the IES-UPM laboratories. The solar simulator has been modified using a large integrating sphere such that it creates a collimated beam in which 90% of the total irradiance is contained within a solid half-angle of  $0.27^\circ$ . The main source of error in this indoor measurement is the non-uniformity of the irradiance created by the solar simulator at the measuring plane (input aperture of the lens). Generally speaking, the level of uniformity depends on the size of the primary optics over which the light is integrated. The Helios 3198 has been reported to attain a uniformity better than  $\pm 5\%$  for  $3 \times 3$  cm optics (Domínguez et al., 2008). The effect of non-uniformity over the efficiency measurement can be critical as it does not only affect the irradiance at the lens aperture but also at the estimation of the input irradiance as the area of the irradiance sensor is significantly smaller. Hence, a previous estimation of the uniformity of the irradiance becomes compulsory to quantify the experimental error. One solution is to map the distribution of light entering the lens with a sensor and calculate the average irradiance.

Usually the nominal focal distance of a lens differs from the distance that actually minimizes the irradiance spot. This is because the nominal focal distance may have been defined for a certain wavelength and it does not correspond to the distance where the spot including all the wavelengths of interest is minimized. Hence, it results useful to conduct several measurements sweeping through several lens-to-receiver distances (see Section 5.2 and Fig. 8). However, if the area of the solar cell used is sufficiently large the effective optical efficiency is independent of the lens-to-receiver distance for positions close to the nominal focal distance. Fig. 4 shows the effective optical efficiency according to Eq. (4) measured for a  $12 \times 12$  cm SOG Fresnel lens at different lens-to-receiver distances. Although the plot shows efficiency vs normalized focal distance, it is an artifact of the measurement only. That is, lens-to-receiver distance is varied only to ensure that we find a position where all rays are captured by the sensor, and therefore find an accurate value of effective optical efficiency. Then, the estimated effective optical efficiency from every focal scan is found as the average of the measured optical efficiencies that are within 0.3% of the maximum value observed. The accuracy of the measured effective optical efficiencies is estimated to be  $\pm 0.02$  based on calculations of error propagation (including known errors and uncertainties). The repeatability of the measurement was determined to be  $\sigma = \pm 0.002$  for measurements performed in the same series (same day). Repeatability is affected by variations due to flash-to-flash deviations as well as errors introduced by the set-up including inaccuracies when mounting the lens.

Additionally, it may be interesting to perform this scan for several lens temperatures, particularly for SOG lenses. There are two options to modify the lens temperature. The first one consists in placing both the lens and the solar cell into a thermal chamber. In this case, the variation in the solar cell spectral response under different temperatures must be considered when estimating the effective lens efficiency. A straightforward way to solve this issue is to place the input irradiance sensor also into the chamber. A second alternative is the use of an enclosure around the lens so that it can be warmed independently of the solar cell (Besson et al., 2016). The wall of the enclosure between the lens and the cell must, of

course, be transparent for all the wavelengths of interest. Obviously, the Fresnel losses at this interface must be discounted to estimate the effective lens efficiency, for example by placing two panels of the same transparent material in front of the input irradiance sensor.

If they are available and meet the requirements listed above, MJ solar cells can be employed to estimate the effective lens efficiency relative to each subcell according to Eq. (5). As previously described, the proposed methods to avoid an erroneous measurement caused by different subcell limitation are either using 'isotype' solar cells and taking advantage of the subcell-limitation diagrams (Domínguez et al., 2013).

Similar approaches to measure the efficiency of a CPV primary lens indoors have been reported. Cotal and Sherif (2005) measured the efficiency of a system comprising a Fresnel lens and a triple junction (3J) solar cell as a function of the lens-to-receiver distance using an ad hoc modified solar simulator. Wiesenfarth et al. (2014) reported outdoor effective lens efficiency measurements using several solar cells as irradiance sensors. They used the efficiency definition of Eq. (4) and employed both 3J solar cell and 'isotype' cells, to estimate the efficiency of several SOG Fresnel lens samples.

#### 4.3. Wavelength resolved efficiency

The spectrally resolved effective optical efficiency  $\eta_{op,eff}(\lambda)$  would provide valuable information for the design and optimization of a CPV module, but it requires the wavelength resolved measurement of both input and output irradiances  $G_{in}(\lambda)$  and  $G_{out}(\lambda)$ . A straightforward way is the use of spectroradiometers (Bengochea et al., 2011), but it has inherent difficulties for CPV optics that we will detail here. Firstly, the aforementioned sources of errors related to non-linearity and non-uniformity of the sensor are worsened here because the spectroradiometer probe is usually smaller than the light spot. Primary lenses suffer such strong chromatic aberration that the spectral irradiance distribution is completely different at the center of the spot or at its rim. The integration of all rays projected by the lens probably requires either a dome-shape diffuser probe or an integrating sphere whose impact in the irradiance distribution must be carefully considered. Additionally, as a result of the chromatic aberration,  $\eta_{op,eff}(\lambda)$  is strongly dependent of the concentration ratio  $X_{geo}$  considered, the focal distance, the lens temperature and the angular deviation between the input beam and the normal to the lens aperture area, so a huge amount of information would we needed to sweep all combinations. Besides the concerns mentioned above related to indoor measurement, using a spectroradiometer entails an additional source of error. The spectroradiometer measures narrow spectral bands by means of band-pass filtering or splitting (e.g., diffraction gratings). The time employed by the instrument in the spectrum splitting makes hardly feasible to measure the spectral irradiance of 1-sun-intensity during a short flash. Therefore, this method can only be applied indoors with continuous simulators or large flash pulses. This last requires very short integration times, and proper time synchronization with the flash pulse, resulting in very expensive equipment when wide broad bands (typically 300–1800 nm) are required.

Considering all these drawbacks, the alternative option of providing a set of effective optical efficiencies for the several subcells involved in MJ cells seems more reasonable. This set of efficiencies, e.g., three for 3 junction cells  $\eta_{op,eff\ top}$ ,  $\eta_{op,eff\ mid}$ , and  $\eta_{op,eff\ bot}$ , make up a three sample spectrally resolved  $\eta_{op,eff}$  this information being easily provided as a function of the focal distance, concentration ratio, angular deviation, temperature and even mechanical tolerances.

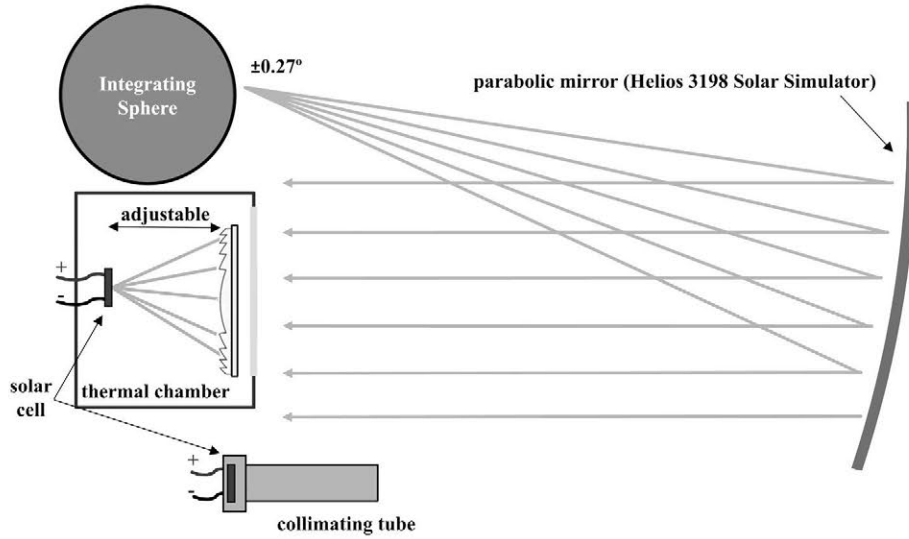


Fig. 2. Scheme of the indoor measuring set-up when using the solar cell as irradiance sensor.

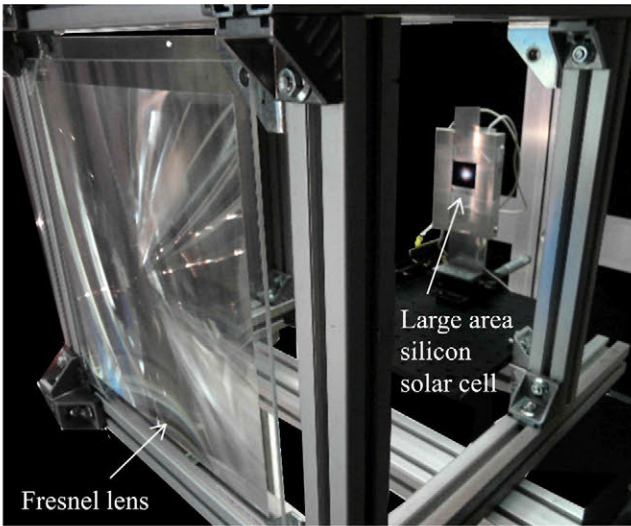


Fig. 3. Indoor measuring set-up at IES-UPM characterization laboratories.

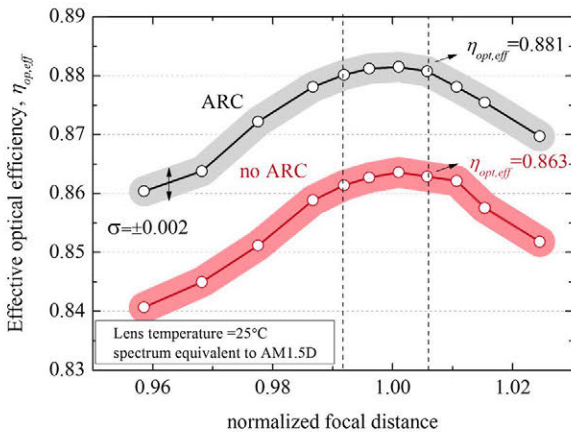


Fig. 4. Effective optical efficiency  $\eta_{opt,eff}$  of a  $12 \times 12$  cm SOG Fresnel lens as defined by equation (4) and measured using a  $2 \times 2$  cm silicon solar cell. The repeatability of the measurement is  $\sigma = \pm 0.002$ . The graph shows the measurement for a lens including antireflective coating (ARC) and a lens without it.

## 5. Characterization of the light spot casted by the lens

The 'encircled energy' is defined as the fraction of the total energy enclosed within circles of increasing radius at the centroid of the receiver. In the case of square solar cells, a more convenient 'ensquared energy' function can be defined as the fraction of power in a square of increasing area. An 'encircled energy' graph is obtained when plotting normalized effective optical efficiency versus cell size. The size of the light spot is determined as the size of the smaller cell from which the efficiency remains constant.

### 5.1. Using solar cells of different sizes

A first method is based on the use of solar cells with different sizes to measure the effective optical efficiency as defined in (4) which has been described in detail elsewhere (Domínguez, 2012). The main limitation is that it requires a set of solar cells which have different but close sizes suitable for the lens to be measured. An alternative solution consists in using photolithographic masks which are transparent within a circle of the radius of interest. All the concerns mentioned in Section 4.2 applies here. In particular, errors due the differences in the effective shading factors caused by the front metallization grid depending on the irradiance profile must be carefully analyzed. A proposed solution to avoid these errors for the case of small lenses consists in using solar cells whose front grid has been removed (Domínguez, 2012). To reduce series resistance a wider and extremely high doped emitter is used. Certainly, with this modifications series resistance is still high but since the short-circuit current is used to estimate the effective optical efficiency, provided that it remains linear, the method is still valid.

### 5.2. Lambertian diffusor and CCD camera

The alternative procedure to quantify the size and shape of the spot is a photograph taken by means of a charge-coupled device (CCD) camera. As previously explained, the solar simulator for CPV Helios 3198 (including the integrating sphere) produces a collimated light beam spectrally matched to AM1.5D (Domínguez et al., 2008) at the aperture of the lens. In this case, the irradiance sensor is replaced by a thin translucent Lambertian diffusing surface and the irradiance distribution at that plane is imaged with a CCD camera. The diffusor allows photographing irradiance

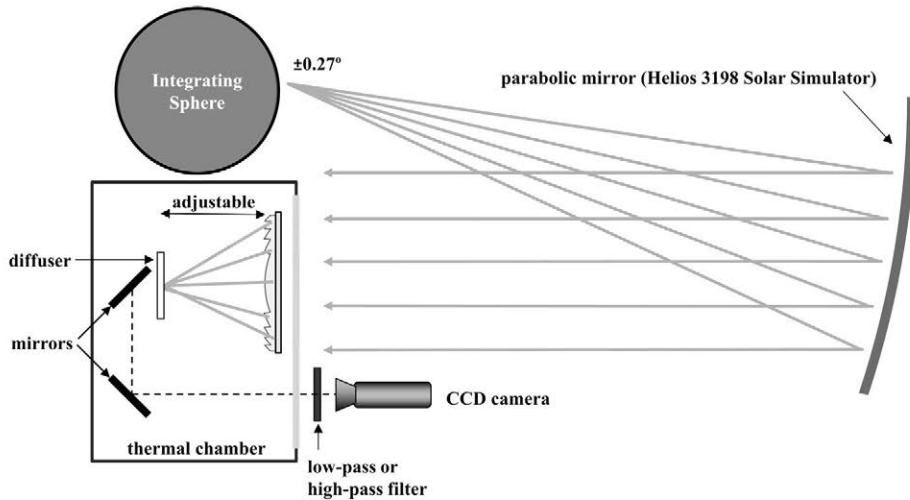


Fig. 5. Scheme of the measuring set-up to estimate the size of the light spot.

distributions larger than the size of the CCD sensor. At the IES-UPM, the set-up includes motorized opto-mechanical stages to allow the quick quantification of the spot size for independently variable lens-to-receiver distances and temperature of the lens. The lens is placed into a thermal chamber with a high-transmission low-iron glass window. Two mirrors are placed at 45° in order to redirect the image of the irradiance profile formed on the diffuser back out of the chamber to the CCD camera (Figs. 5 and 6).

By using adequate filters, the irradiance profile of the spectral band 'seen' by a particular subcell of a MJ cell can be recorded separately. Differences in the spectral response of the camera plus filters assembly and the subcells may introduce some errors mainly if the SR limits for each case are distinct. As an example case, the combined spectral response of a silicon CCD sensor and a cut-off low-pass and high-pass filter respectively are shown in Fig. 7, in comparison to the top and middle spectral response of a lattice match GaInP/InGaAs/Ge triple junction cell. It should be remarked here that the irradiance profile 'seen' by the bottom subcell cannot be measured since the silicon sensor in the CCD camera cannot detect light at the wavelengths this subcell is sensitive to. However, for the majority of optical materials, dispersion is far more significant at shorter wavelengths than at longer ones, hence the bottom subcell irradiance profile is far more similar to the middle subcell irradiance profile than the middle is to the top. This, along with the fact that bottom subcell in classic germanium based MJ solar cell generates an excess of current, diminishes the importance of this limitation.

This measurement does not provide an absolute value of the irradiance since it would need a calibration of the whole set-up, including filters, CCD camera and diffuser. Nevertheless, the wide dynamic range of the CCD sensors allows an accurate comparison between the peak and valley values over an image. The diffuser must have a Lambertian response to avoid altering the intensity map. Several materials are suitable to manufacture a good Lambertian surface, e.g., magnesium oxide deposited over ground glass, Teflon or Spectralon (sintered polytetrafluoroethylene, PTFE). The diffuser must feature fiducial marks at a known distance for determining the pixels-to-mm calibration of the CCD image, and should be large enough to ensure that significant "dark" areas are present. The calculation of the irradiance spot is as follows. First, the background noise (given at dark areas) is removed from the image. Second, the centroid of the luminous spot is found, and then a radial irradiance profile is calculated by averaging the irradiance in

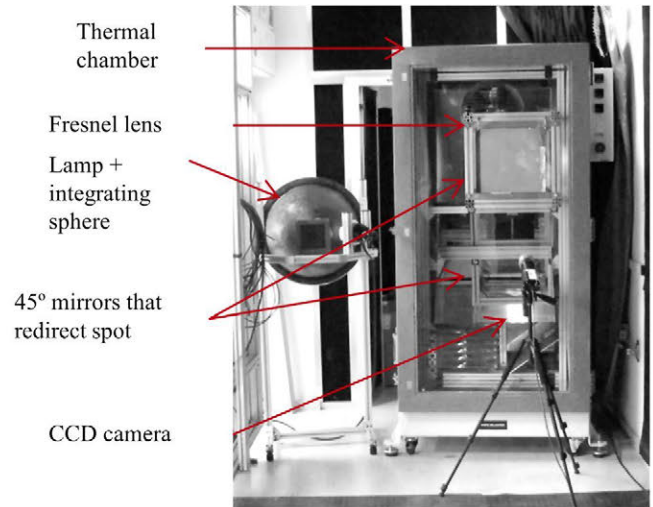


Fig. 6. Measuring set-up at IES-UPM characterization lab.

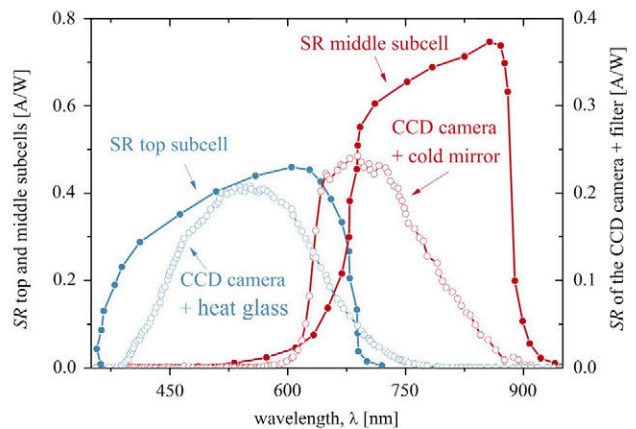
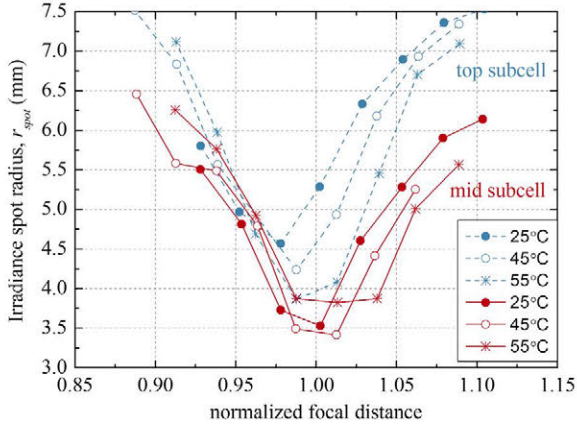
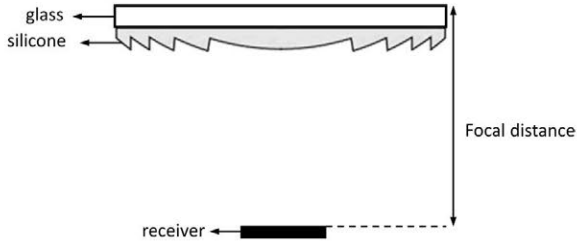


Fig. 7. Spectral response SR, of the CCD camera silicon sensor filtered by a cold mirror or a heat glass (empty dots) to simulate the SR of middle and top subcells of a 3 J lattice-matched solar cell (solid dots).



**Fig. 8.** Size of the irradiance spot corresponding to top and middle subcells for a  $12 \times 12$  cm SOG Fresnel lens measured at different temperatures using the Lambertian diffusor and CCD camera method. Due to chromatic aberration the focal distance where spot minimizes is longer for the wavelengths range of the middle subcell than for the top. As the temperature increases the refractive index of the silicone decreases and the position where the spot is minimum moves further from the lens.



**Fig. 9.** Definition of focal distance in the measurements.

concentric rings (or squares) of pixels around the centroid (Fig. 11). This profile is integrated to find the irradiance spot radius (or half-width of the square) that encircles 95% of the total flux which is considered to be the radius of the light spot  $r_{spot}$  (Antón et al., 2003). The effective concentration ratio  $X_{spot}$  is obtained dividing the lens aperture area  $A_{in}$  by the area of the light spot.

$$X_{spot} = \frac{A_{in}}{\pi r_{spot}^2} \quad (6)$$

This procedure provides the spatial distribution of the irradiance at the receiver plane (i.e., focal plane) which gives information about its deviation from the ideal behavior (for example

given by ray-tracing simulations). Strong differences in shape with the expected profile indicate either imperfections in the optical surfaces (as roughness or bending) or in the assembly process (producing misalignments). Furthermore, the method allows the estimation of non-uniform photocurrent distribution in every subcell within a MJ solar cell. This information results crucial to analyze the losses in the electrical efficiency of a system (comprising the lens under evaluation) due to low fill factor caused by high effective series resistance (Espinete, 2012; Herrero et al., 2012; Kurtz and O'Neill, 1996; Victoria et al., 2013) and to current losses due to high lateral resistance. Of course the method can be used to evaluate both classic imaging lenses and non-imaging lenses.

Fig. 8 shows an example of this method. The size of the irradiance spots for a  $12 \times 12$  cm SOG Fresnel lens at different temperatures is shown. Additionally, there are several publications (Antón et al., 2003; Herrero et al., 2012; Askins et al., 2011) that reproduce results obtained with this method.

A similar approach has been used by other researchers to quantify the spot cast by a primary lens. Indoors measurement using a CPV solar simulator based on refractive optics were conducted in the Photovoltaics Laboratory at the Ioffe Institute (Shvarts et al., 2008). Indoor measurements using monochromatic light were reported by researchers at the Fraunhofer ISE (Nitz et al., 2007; Hornung et al., 2010).

## 6. Example of the optical characterization of a lens

This section summarizes all the data that could be provided as a result of a complete characterization of a Fresnel lens to be used as primary element of a CPV system. Focal distance is defined as the distance (from the first surface of the lens where light impinges to the receiver plane, see Fig. 9) where the effective concentration ratio is maximum. In addition to the data gathered in Table 3 the following information could be graphically depicted: irradiance distribution on the receiver (Fig. 10), encircled energy (Fig. 11), spot radius at several temperatures and focal distances (Fig. 12) and focal distance dependence with temperature for different wavelength bandwidths (Fig. 13).

## 7. Discussions and conclusions

In the previous sections we have presented a wide review of different methods to evaluate the lens performance and to estimate the optical efficiency of a primary lens. It is difficult to determine the most appropriate as probably each of them is the best for measuring a particular feature of the lens and the chosen procedure depends on the specific objective. Nevertheless the purpose of this

**Table 3**  
Dimensional and optical parameters.

Aperture area, $A_{in}$	$120 \times 120$	mm	
Effective optical efficiency, $\eta_{op,eff}$ AM1.5D, 25 °C, silicon [300, 1150]	$0.881 \pm 0.002$		Section 4.2
Irradiance spot radius, $r_{spot}$ (95% total flux) AM1.5D, 25 °C, [375, 900]	4.2	mm	Section 5.2
Effective concentration ratio, $X_{spot}$ (for $r_{spot}$ ) AM1.5D, 25 °C, [375, 900]	260		Section 5.2
Focal distance, AM1.5D, 25 °C			
Top subcell [375, 700]	194.8	mm	
Middle subcell [600, 900]	198.2	mm	Section 5.2
[375,900]	197.4	mm	
Focal distance temperature coefficient			
Top subcell [375, 700]	0.14	mm/°C	
Middle subcell [600, 900]	0.16	mm/°C	Section 5.2
[375,900]	0.15	mm/°C	



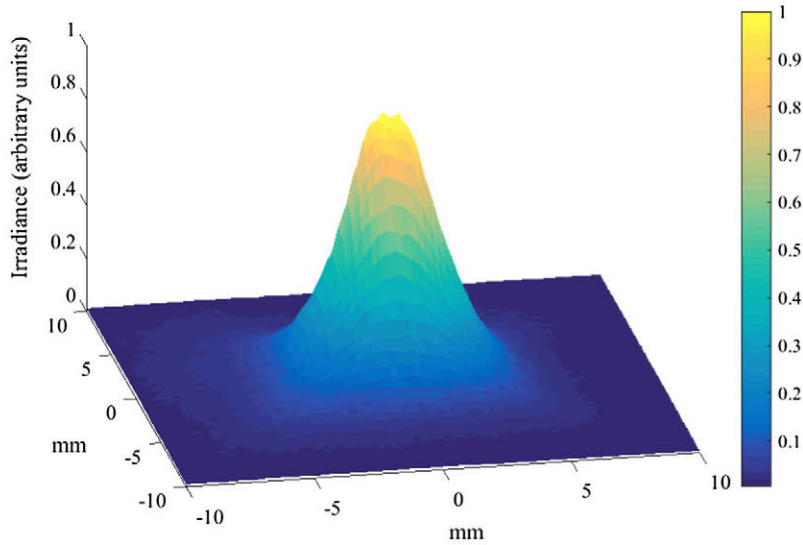


Fig. 10. Irradiance distribution on the receiver. AM1.5D, 25 °C, [375, 900], Focal distance 197.4 mm.

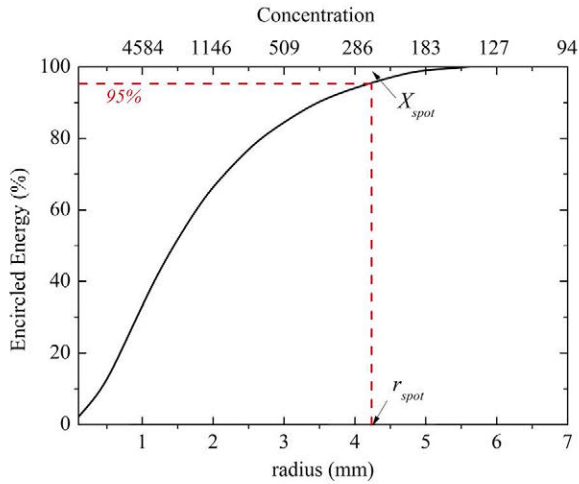


Fig. 11. Encircled energy. Ratio of the total irradiance contained in a circle of a certain radius.

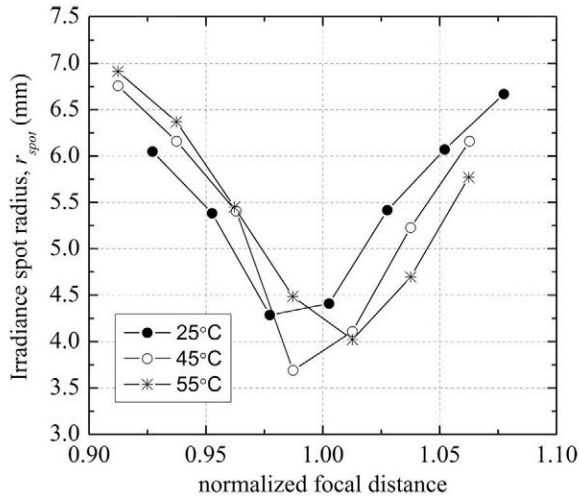


Fig. 12. Irradiance spot radius measured at different temperatures using the Lambertian diffusor and CCD camera method. AM1.5D, [375, 900].

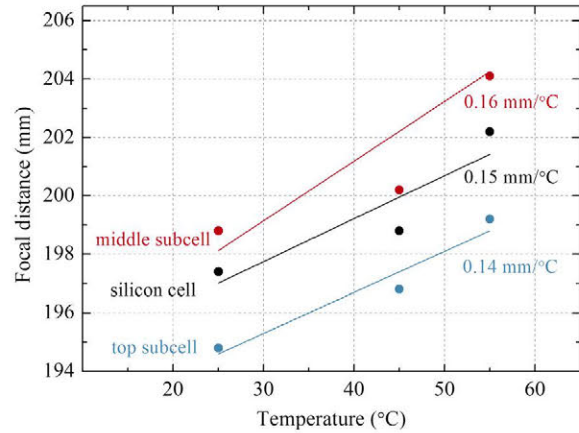


Fig. 13. Focal distance vs. temperature. Data has been obtained from Figs. 8 and 12.

text is to identify the most suitable method to determine the efficiency of a primary lens to be used in a CPV system, that is, we want either to check the quality of the lens manufacture, to compare different lenses, or to provide the performance characteristics of a primary lens that will be integrate in a system. In other words, the results of the measurements may serve for optics designers, manufactures and CPV designers to agree. For this purpose, based on previous experience at IES-UPM, and taking into account the availability of irradiance sensors we proposed using methods 4.2 and 5.2, i.e., using a large area solar cell to determine the effective lens optical efficiency and the CCD camera to measure the size of the light spot.

The combination of these two methods allows a comprehensive characterization of a lens sample. On the one hand, using a solar cell as sensor enables the detection of deficiencies in the lens transmittance, e.g., high-absorbing silicone, degraded PMMA, high Fresnel losses in any of the surfaces, losses due to large draft angles or tip rounding, etc. On the other hand, the CCD camera method allows the evaluation of the lens capability to concentrate light within the wavelengths of interest, providing detailed information about its suitability for a given CPV system.

## Acknowledgements

This work has been partially supported by the Spanish Ministry of Economy and Competitiveness under the Acromalens project (ENE2013-45229-P) and the MadridPV project (S2013/MAE2780) founded by the Comunidad de Madrid.

- Antón, I., Pachón, D., Sala, G., 2003. Characterization of optical collectors for concentration photovoltaic applications. *Prog. Photovolt. Res. Appl.* 11, 387–405. <http://dx.doi.org/10.1002/pip.502>.
- Askins, S., Victoria, M., Herrero, R., Domínguez, C., Antón, I., Sala, G., 2011. Effects of temperature on hybrid lens performance. *AIP Conf. Proc.* 1407, 57–60. <http://dx.doi.org/10.1063/1.3658294>.
- Bengoechea, J., Ezquer, M., Petrina, I., Lagunas, A.R., 2011. Experimental set-up to evaluate the degradation of the optical components of a CPV module. *AIP Conf. Proc.* 1407, 84–87. <http://dx.doi.org/10.1063/1.3658300>.
- Besson, P., White, P.M., Domínguez, C., Voarino, P., Garcia-Linares, P., Lemiti, M., Schriemer, H., Hinzer, K., Baudrit, M., 2016. Spectrally-resolved measurement of concentrated light distributions for Fresnel lens concentrators. *Opt. Express* 24, A397–A407. <http://dx.doi.org/10.1364/OE.24.00A397>.
- Chai, A.T., 1976. Some basic considerations of measurements involving collimated direct sunlight. Presented at the 2nd Annual Photovoltaic Measurements Workshop.
- Cotal, H., Sherif, R., 2005. The effects of chromatic aberration on the performance of GaInP/GaAs/Ge concentrator solar cells from Fresnel optics. Presented at the 31st IEEE Photovoltaic Specialists Conference, pp. 747–750. <http://dx.doi.org/10.1109/PVSC.2005.1488240>.
- Domínguez, C., 2012. Optical and electrical characterization of high-concentration photovoltaic systems. Universidad Politécnica de Madrid.
- Domínguez, C., Antón, I., Sala, G., 2008. Solar simulator for concentrator photovoltaic systems. *Opt. Express* 16, 14894–14901. <http://dx.doi.org/10.1364/OE.16.014894>.
- Domínguez, C., Antón, I., Sala, G., Askins, S., 2013. Current-matching estimation for multijunction cells within a CPV module by means of component cells. *Prog. Photovolt. Res. Appl.* 21, 1478–1488. <http://dx.doi.org/10.1002/pip.2227>.
- Espinete, P., 2012. Advances in the modelling, characterization and reliability of concentrator multijunction solar cells. Universidad Politécnica de Madrid.
- Herrero, R., Victoria, M., Domínguez, C., Askins, S., Antón, I., Sala, G., 2012. Concentration photovoltaic optical system irradiance distribution measurements and its effect on multi-junction solar cells. *Prog. Photovolt. Res. Appl.* 20, 423–430. <http://dx.doi.org/10.1002/pip.1145>.
- Hornung, T., Bachmaier, A., Nitz, P., Gombert, A., Bett, A.W., Dimroth, F., 2010. Temperature dependent measurement and simulation of Fresnel lenses for concentrating photovoltaics. *AIP Conference Proceedings*. Presented at the CPV-6, Freiburg, Germany, pp. 85–88. <http://dx.doi.org/10.1063/1.3509239>.
- Kurtz, S.R., O'Neill, M.J., 1996. Estimating and controlling chromatic aberration losses for two-junction, two-terminal devices in refractive concentrator systems. Presented at the 25th IEEE Photovoltaic Specialists Conference, pp. 361–364. <http://dx.doi.org/10.1109/PVSC.1996.564020>.
- Nitz, P., Heller, A., Platzer, W.J., 2007. Indoor characterisation of Fresnel type concentrator lenses. Presented at the 4th Conference on Solar Concentrators for the Generation of Electricity or Hydrogen, El Escorial, Spain.
- Rumyantsev, V.D., Davidiyuk, N.Y., Ionova, E.A., Pokrovskiy, P.V., Sadchikov, N.A., Andreev, V.M., 2010. Thermal regimes of Fresnel lenses and cells in "All-Glass" HCPV modules. *AIP Conf. Proc.* 1277, 89–92. <http://dx.doi.org/10.1063/1.3509240>.
- Shvarts, M.Z., Andreev, V.M., Gorohov, V.S., Grilikhes, V.A., Petrenko, A.E., Soluyanov, A.A., Timoshina, N.H., Vlasova, E.V., Zaharevich, E.M., 2008. Flat-plate Fresnel lenses with improved concentrating capabilities: designing, manufacturing and testing. Presented at the 33rd IEEE Photovoltaic Specialists Conference, pp. 1–6. <http://dx.doi.org/10.1109/PVSC.2008.4922751>.
- Victoria, M., Domínguez, C., Antón, I., Sala, G., 2009. Comparative analysis of different secondary optical elements for aspheric primary lenses. *Opt. Express* 17, 6487–6492. <http://dx.doi.org/10.1364/OE.17.006487>.
- Victoria, M., Herrero, R., Domínguez, C., Antón, I., Askins, S., Sala, G., 2013. Characterization of the spatial distribution of irradiance and spectrum in concentrating photovoltaic systems and their effect on multi-junction solar cells. *Prog. Photovolt. Res. Appl.* 21, 308–318. <http://dx.doi.org/10.1002/pip.1183>.
- Wiesenfarth, M., Steiner, M., Wolf, J., Schmidt, T., Bett, A.W., 2014. Investigation of different Fresnel lens designs and methods to determine the optical efficiency. *AIP Conf. Proc.* 1616, 97–101. <http://dx.doi.org/10.1063/1.4897037>.